the FEBS Journal

Evidence for β-lactoglobulin involvement in vitamin D transport *in vivo* – role of the γ-turn (Leu-Pro-Met) of β-lactoglobulin in vitamin D binding

Ming Chi Yang[1], Nai Chi Chen[1], Chun-Jung Chen[2,3], Chin Yun Wu[1] and Simon J. T. Mao[1,4]

1 Department and College of Biological Science and Technology, National Chiao Tung University, Taiwan
2 Life Science Group, Research Division, National Synchrotron Radiation Research Center, Taiwan
3 Department of Physics, National Tsing Hua University, Taiwan
4 Department of Biotechnology and Bioinformatics, Asia University, Taichung, Taiwan

Keywords
β-lactoglobulin; monoclonal antibody; site-directed mutagenesis; vitamin D binding; vitamin D transport and uptake

Correspondence
S. J. T. Mao, Department of Biological Science and Technology, College of Biological Science and Technology, National Chiao Tung University, 75 Po-Ai Street, Hsinchu 30050, Taiwan
Fax: +886 3 572 9288
Tel: +886 3 571 2121 (ext. 56948)
E-mail: mao1010@ms7.hinet.net

(Received 9 December 2008, revised 3 February 2009, accepted 6 February 2009)

doi:10.1111/j.1742-4658.2009.06953.x

β-lactoglobulin (LG) is a major bovine milk protein, containing a central calyx and a second exosite beyond the calyx to bind vitamin D; however, the biological function of LG in transporting vitamin D remains elusive. Crystallographic findings from our previous study showed the exosite to be located at the pocket between the α-helix and β-strand I. In the present study, using site-directed mutagenesis, we demonstrate that residues Leu143, Pro144 and Met145 in the γ-turn loop play a crucial role in the binding. Further evidence is provided by the ability of vitamin D_3 to block the binding of a specific mAb in the γ-turn loop. Using the mouse (n = 95) as an animal model, we initially demonstrated that LG is a major fraction of milk proteins responsible for uptake of vitamin D. Most interestingly, dosing mice with LG supplemented with vitamin D_3 revealed that native LG containing two binding sites gave a saturated concentration of plasma 25-hydroxyvitamin D at a dose ratio of 2 : 1 (vitamin D_3/LG), whereas heated LG containing one exosite (lacking a central calyx) gave a ratio of 1 : 1. We have demonstrated for the first time that LG has a functional advantage in the transport of vitamin D, indicating that supplementing milk with vitamin D effectively enhances its uptake.

Bovine β-lactoglobulin (LG) is a major whey protein that constitutes 10–15% of the total proteins in bovine milk [1]. Since the 1960s, the thermally unstable and molten globule nature of LG has stimulated extensive research into its physical and biochemical properties [2–10]. The crystal structure of LG, which is well established [11,12], has been used mostly as a benchmark to predict the secondary structure of a given protein with a known amino acid sequence [13]. As shown in Fig. 1A, the protein has predominantly a β-sheet conformation containing nine antiparallel β-strands from A to I. Topographically, β-strands A–D form one surface of the barrel (calyx), and β-strands E–H form the other [14–16]. The calyx has a remarkable ability to bind hydrophobic molecules such as retinol, fatty acids, and vitamin D [17–20]. According to a crystallographic structure of the LG–vitamin D_3 complex (Fig. 1B) [9,10], the α-helical region with three turns linking with β-strand I on the surface is involved in binding vitamin D at the secondary exosite. The conformational changes of LG upon heating are rapid and extensive above the transition temperature (~ 70 °C), at which β-strand D of the calyx participates in the unfolding during thermal denaturation [6]. As a result, thermal treatment diminishes the calyx binding site for palmitate or retinol, but does not affect the exosite for vitamin D binding [6,9,10]. In our previous study, we proposed that this exosite contains a unique inverse

Abbreviations
LG, β-lactoglobulin; rLG, recombinant β-lactoglobulin; SD, standard deviation.

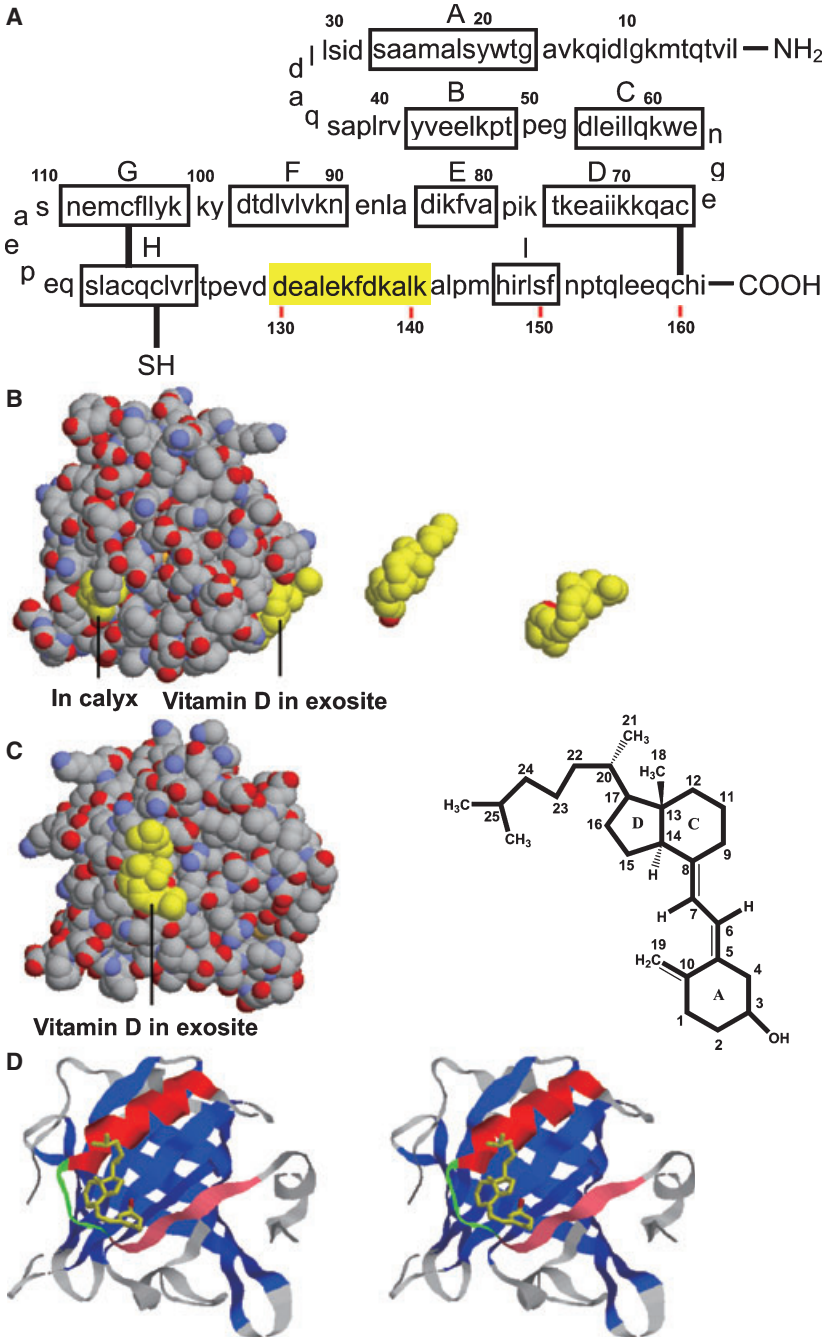

Fig. 1. Amino acid sequence of LG and crystal structure of the LG–vitamin D_3 complex. (A) LG comprises 162 amino acids with nine β-sheet strands (A–I). The α-helix with three turns is located between residues 130 and 141 (yellow). (B) Space-filling drawing of the LG–vitamin D_3 complex at 2.4 Å resolution. Vitamin D_3 (carbon yellow and oxygen red) and LG are drawn on the basis of our previously refined model [9,10], with one vitamin D_3 molecule penetrating inside the calyx (left) and the other lying on the surface pocket at the C-terminus (residues 136–149) (right). (C) Front view of vitamin D_3 binding to the exosite and chemical structure of vitamin D_3. (D) The 3D ribbon model of the LG–vitamin D_3 complex shows that the exosite combines an α-helix (red) and β-strand I (pink) with a γ-turn loop (green). (A) and (B) are reproduced from our previous study [9], with permission of the publisher.

γ-turn loop (residues 143–145 or Leu-Pro-Met), located between the α-helix and β-strand I, that is essential in forming a pocket to bind vitamin D [9].

In the present study, we expressed recombinant LG (rLG) in *Escherichia coli*, and used site-directed mutagenesis to produce a set of mutants to test the hypothesis that this γ-turn plays an essential role in the interaction between LG and vitamin D. We further tested this hypothesis using a mAb specific for this γ-turn region (selected from a battery containing 900 mAbs) as a probe, and then determined whether vitamin D might interfere with the binding between LG and the mAb. In addition, although the binding of vitamin D to milk LG is well known [9,10,14,21,22], whether it enhances the transport of vitamin D of milk is still unproven.

We have demonstrated for the first time that LG is a fraction responsible for the uptake of vitamin D_3 from milk, using the mouse (n = 95) as an animal model. Most interestingly, we showed that native LG

containing both the calyx and exosite had an efficacy in vitamin D_3 uptake almost twice that of heated LG containing a single exosite. Our study therefore provides new insights concerning the value of supplementing dairy products with vitamin D.

Results

Overall crystal structure of the LG–vitamin D_3 complex

Our space-filling drawing of the LG–vitamin D_3 complex at 2.4 Å resolution reveals two domains in which vitamin D_3 is bound (Fig. 1B). One vitamin D_3 molecule inserts almost perpendicularly into the calyx cavity with the 3-OH near the outside similar to that of retinol binding; the other binds to the exosite near the C-terminus of LG (residues 136–149), including a γ-turn loop (residues 143–145) by combining part of the α-helix and β-strand I (Fig. 1C,D). [Correction added on 18 March 2009 after first online publication: in the preceding sentence, 'One vitamin D_3 molecule inserts almost perpendicularly into the calyx cavity with the 3-OH near the outside similar to that of retinol binding;' has been inserted.] Uniquely, the α-helix in the exosite is totally amphipathic, as pointed out previously [23], with one face totally comprising charged amino acid residues, and another face totally comprising hydrophobic residues (Fig. 2A). The A-ring and the aliphatic tail of vitamin D_3 (following the C/D-rings) interact with β-strand I and the α-helix of LG, respectively (Fig. 1D). The crystal structure of the LG–vitamin D_3 complex shows clearly that the conformation of vitamin D_3 differs significantly between the two binding sites (Fig. 1B). This fact explains why fatty acid and retinol are unable to bind at the secondary exosite. In the first phase of the present study, we tested the hypothesis that a γ-turn loop is essential to allow a stable interaction between vitamin D and the exosite (Fig. 1D) [9], using LG mutants produced from *E. coli*.

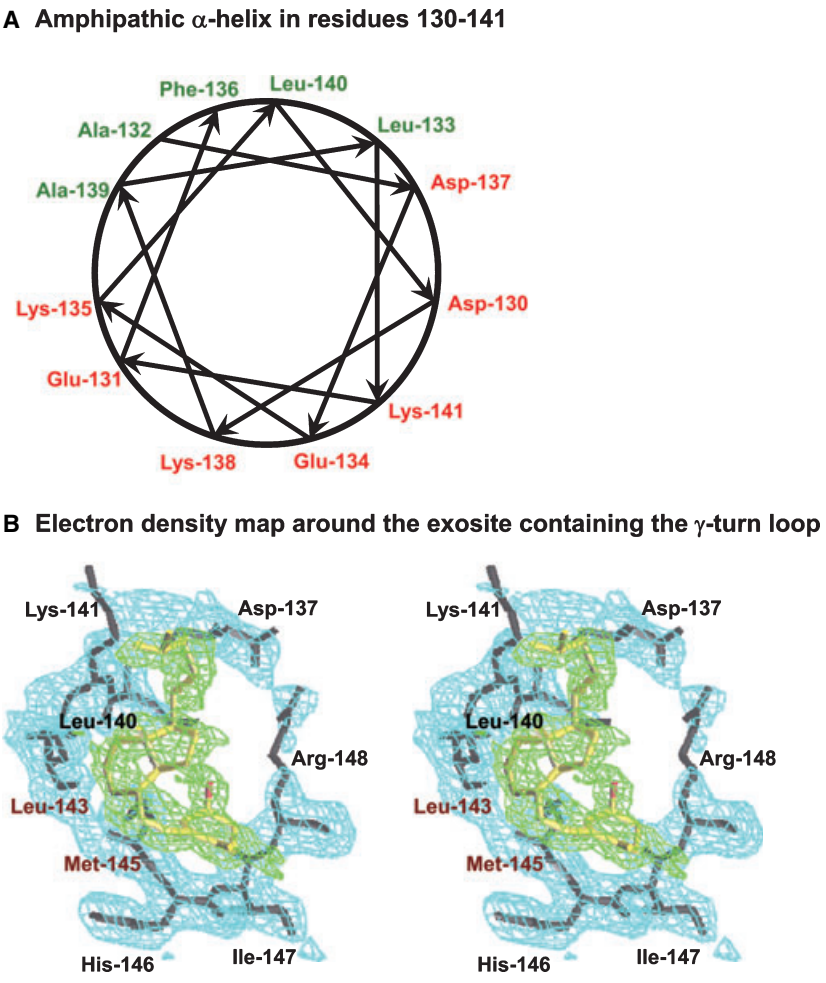

Fig. 2. Amphipathic α-helix of LG and its interaction with vitamin D_3. (A) Unique amphipathic α-helix of LG. (B) Final refined model with the $2|F_{obs} - F_{calc}|$ electron density showing that the bulk of the density is sufficient to cover the vitamin D_3 in the exosite. The figures are reproduced from our previous study [9], with permission of the publisher.

Expression, purification and western blot of rLG and its mutants

Figure 3A shows that each rLG or mutant was abundantly expressed, with the average expression levels being approximately 30% of that of total lysate proteins. As each mutant contains a 6× His-tag, the molecular mass (~ 19.7 kDa) was slightly greater than that (18.4 kDa) of native LG. Each purified recombinant protein showed ~ 95% homogeneity in reducing SDS/PAGE, and this was verified with a western blot using a LG-specific mAb (4D11) [6] (Fig. 3B).

Vitamin D_3 binding to LG and rLG

To determine whether rLG was capable of interacting with vitamin D in a manner similar to that of native LG, we monitored the quenching of Trp fluorescence for the binding according to an established method [6,9,10,21,22]. Figure 4A and Table 1 show that maximal vitamin D_3 binding to native LG was achieved at a ratio of 2 : 1, but that the binding to rLG remained at a ratio of 1 : 1. The expressed rLG hence incompletely mimics the native LG structure with a loss of one vitamin D binding site or partial loss for both sites. Because palmitate and retinol bind to only the central calyx, not to the exosite [18], we used each of these two ligands as a 'marker' to monitor whether they still interact with rLG. The results revealed that neither palmitate nor retinol interact with rLG, as judged by the absence of Trp fluorescence changes (Table 1), indicating that the correct conformation of the central calyx was not present in rLG.

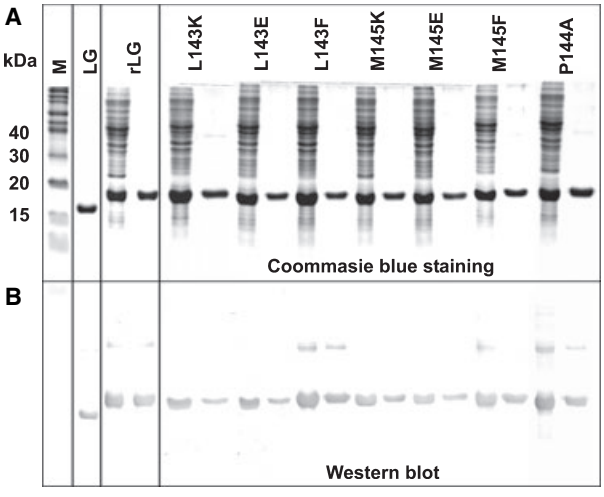

Fig. 3. Expression and purification of recombinant LG and its mutants from *E. coli*. (A) SDS/PAGE (in the presence of mercaptoethanol) of native LG isolated from milk, cell lysate (paired left), and isolated rLG (paired right). (B) Western blot of cell lysate and isolated rLG mutants using a LG-specific mAb (4D11). M represents a molecular marker.

Figure 4A shows, however, that the exosite seems to be unaltered in rLG, as the binding ratio for vitamin D_3 remained at 1 : 1. Because heat treatment results in a loss of the central calyx but retention of the exosite [6,9,10], we used heated LG (100 °C for 16 min) as a probe to compare its vitamin D_3 binding to rLG. The binding of heated LG attained a ratio of 1 : 1, similar to previous findings [9,10]. Interestingly, the ratios of vitamin D_3 binding to either heated LG or rLG were almost indistinguishable, and heat had no effect on rLG (Fig. 4A, left panel). The affinities of heated LG, heated rLG and rLG for vitamin D_3 were also similar (Fig. 4A, right panel). The number of vitamin D_3-binding sites predicted with a Cogan plot and the apparent dissociation constant calculated from the slope (Fig. 4A, right panel) are listed in Table 1. The binding affinity of native LG (containing two binding sites) was about 5 nM (K_d^{app} = 4.7 ± 0.37 nM), which appears to be seven times that of rLG (containing exosite only) (K_d^{app} = 33.1 ± 3.62 nM).

Because the β-structure of LG is required to maintain the calyx [6,9], we expected its structure to be altered in rLG. From analysis of the CD spectra, we verified the change of the typical β-structure in rLG according to a leftward shift of a symmetric dip at 215 nm characteristic of native LG (Fig. 5A). Heat produced essentially no additional structural change in rLG. There was a minor difference in the CD spectra between heated LG and rLG, which might be due to the presence of the His-tag in the rLG or to different disulfide linkages, described below. Notably, addition of vitamin D_3 to all LG species did not alter the overall CD spectra (data not shown). To confirm the loss of β-structure in expressed rLG, we used a β-structure-dependent specific LG monoclonal antibody (4H11E8) [8] to show that it recognized only native LG, not rLG, on a native gel western blot (Fig. 5B).

Further characterization of rLG using MALDI-TOF and carboxymethylation

Recombinant LG apparently cannot fold to its native state in the *E. coli* expression system, which is a general issue when utilizing a given recombinant protein for the investigation of a structure–function relationship. In our case, the loss of the binding nature of the central calyx in rLG is probably due to the overall change in the β-structure (Fig. 5). Although the exact mechanism involved in such a change remains elusive, we attempted to further investigate whether the disul-

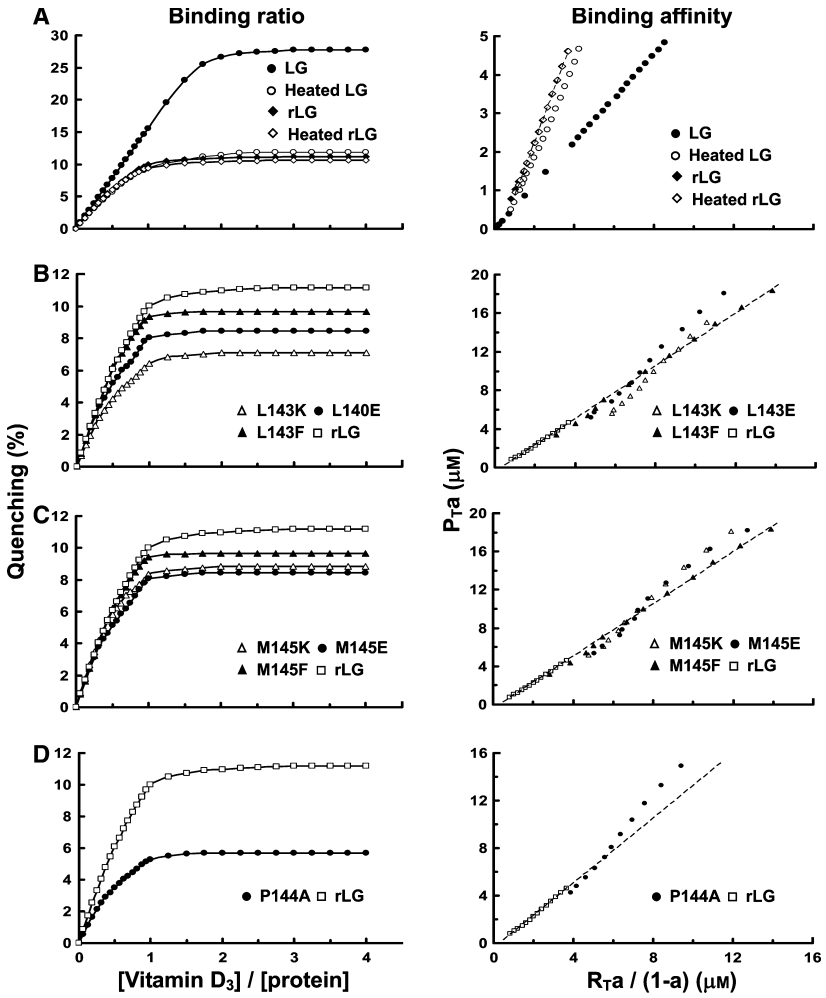

Fig. 4. Fluorescence titration curves of native and heated LG, nonheated and heated rLG or rLG mutants with vitamin D_3. Left panel: titration curve of native LG, heated LG, rLG and heated rLG (A) and mutants (B–D) with vitamin D_3. Right panel: Cogan plot per titration curve. P_T = total protein concentration, R_T = total ligand concentration, and a = fraction of unoccupied ligand sites on the protein. The dashed line in each right-hand panel represents the titration plot of rLG only, used for reference. Each point represents the mean of triplicate determinations. The average SD was less than 5–8% of the mean.

fide linkages (n = 2 from a total of five Cys residues with one free −SH group at position 121 in native LG) are related. The use of limited trypsin-digested fragments of native, heated and recombinant LG in MALDI-TOF analysis revealed (Fig. 6A–D) that rLG contained two complicated intramolecularly crosslinked fragments, including Trp61–Lys69:Tyr102–Arg124 and Tyr 102–Arg124:Leu149–Ile 162 for Cys66–Cys106, Cys66–Cys119, or Cys66–Cys121, and Cys106–Cys160, Cys119–Cys160, or Cys121–Cys160, respectively, that differed from that of native LG, containing Trp61–Lys69:Leu149–Ile162 for Cys66–Cys160. There was an additional crosslinked fragment in heated LG shown by Trp61–Lys69:Tyr102–Arg124 for Cys66–Cys106, Cys66–Cys119, or Cys66–Cys121.

To elucidate the complicated crosslinked species of rLG (for example, dimerization was seen in both heated and recombinant LG), we irreversibly reduced all linkages by carboxymethylation using iodoacetic acid. Under these conditions, we found that native LG, heated LG and rLG were able to form monomers with almost the same homogeneity (Fig. 6E). Interestingly, both carboxymethylated rLG and carboxymethylated heated LG had similar binding ratios (1 : 1) and affinities for vitamin D_3 to those without carboxymethylation, whereas carboxymethylated LG also exhibited a 1 : 1 ratio. Further heating of modified proteins did not affect the binding ratios (Table 1). These results indicate that disulfide linkages are essential to maintain the necessary conformation of the central calyx, but are probably not particularly critical for exosite binding. The expressed rLG therefore provided us with a tool in the subsequent mutant tests involving monitoring of a single exosite interaction.

Vitamin D_3 binding to rLG mutants of γ-turn loop residues 143–145

According to the crystal structure of the LG–vitamin D_3 complex [9], there is a direct interaction

Table 1. Apparent dissociation constants and ratios for binding of ligands to native LG and rLG.

Ligand	Protein	Binding ratio calculated from Cogan plot (ligand/LG)	K_d^{app} Apparent dissociation constant (10^{-9} M)
Vitamin D_3	Native LG	1.76 ± 0.12	4.7 ± 0.37
	Heated LG	0.84 ± 0.05	45.7 ± 3.12
	rLG	0.73 ± 0.03	33.1 ± 3.62
	Heated rLG	0.72 ± 0.02	38.6 ± 3.56
	Carboxymethylated LG[a]	0.84 ± 0.02	35.2 ± 2.92
	Carboxymethylated heated LG[a]	0.84 ± 0.05	39.2 ± 3.08
	Carboxymethylated rLG[a]	0.79 ± 0.03	32.8 ± 3.61
	Carboxymethylated LG with heat treatment[a]	0.83 ± 0.02	35.2 ± 3.03
	Carboxymethylated heated LG with heat treatment[a]	0.83 ± 0.03	40.0 ± 2.38
	Carboxymethylated rLG with heat treatment[a]	0.78 ± 0.03	33.1 ± 3.41
Retinol	Native LG	0.91 ± 0.09	17.3 ± 1.62
	Heated LG	–[b]	–
	rLG	–	–
	Heated rLG	–	–
	Carboxymethylated LG	–	–
	Carboxymethylated heated LG	–	–
	Carboxymethylated rLG	–	–
	Carboxymethylated LG with heat treatment	–	–
	Carboxymethylated heated LG with heat treatment	–	–
	Carboxymethylated rLG with heat treatment	–	–
Palmitate	Native LG	0.80 ± 0.072	44.0 ± 4.56
	Heated LG	–	–
	rLG	–	–
	Heated rLG	–	–
	Carboxymethylated LG	–	–
	Carboxymethylated heated LG	–	–
	Carboxymethylated rLG	–	–
	Carboxymethylated LG with heat treatment	–	–
	Carboxymethylated heated LG with heat treatment	–	–
	Carboxymethylated rLG with heat treatment	–	–

[a] The titration experiment was conducted as for other proteins, but is not shown in Fig. 4. [b] No fluorescence change or no binding in titration experiments.

between vitamin D_3 and the side chains of Leu143 and Met145 in the γ-turn loop, because the distance between vitamin D_3 and each side chain is < 3.8 Å (Figs 1D and 2B). We replaced each of these two residues with a positively charged Lys, a negatively charged Glu, or a hydrophobic Phe, by site-directed mutagenesis. The effect on the binding to vitamin D_3, determined by fluorescence quenching, is shown in Fig. 4B (left and right panels) and Table 2. A markedly decreased binding affinity was seen when Leu143 was substituted with Lys or Glu (8.11-fold or 5.84-fold). Interestingly, there was only a slight decrease when it was replaced by a hydrophobic Phe (0.96-fold) (Fig. 4B). A consistent pattern was likewise seen with the M145K, M145E and M145F mutants upon binding vitamin D_3 (Fig. 4C).

Because Pro is typically found in a γ-turn, we tested the importance of Pro144 using the P144A mutant. Figure 4D and Table 2 show significantly decreased binding of vitamin D_3 (4.6-fold) by the P144A mutant. Table 2 shows that the effects of these residues in the loop region for vitamin D_3 interaction rank overall as Leu143 > Met145 > Pro144.

Interference of vitamin D_3 to γ-turn specific mAb (1D8F8) binding with LG

To select a mAb that might recognize the γ-turn region, we screened a LG mAb battery (n = 900) [5], using a set of mutants as a probe. We found one LG mAb, 1D8F8, that was capable of reacting with the M145K, M145E and M145F mutants, but not with the L143K, L143E and P144A mutants, according to a western blot analysis (Fig. 7A). MAb 1D8F8 is therefore specific for Leu143 and Pro144 located within the γ-turn loop. As Leu143 and Pro144 are located inside

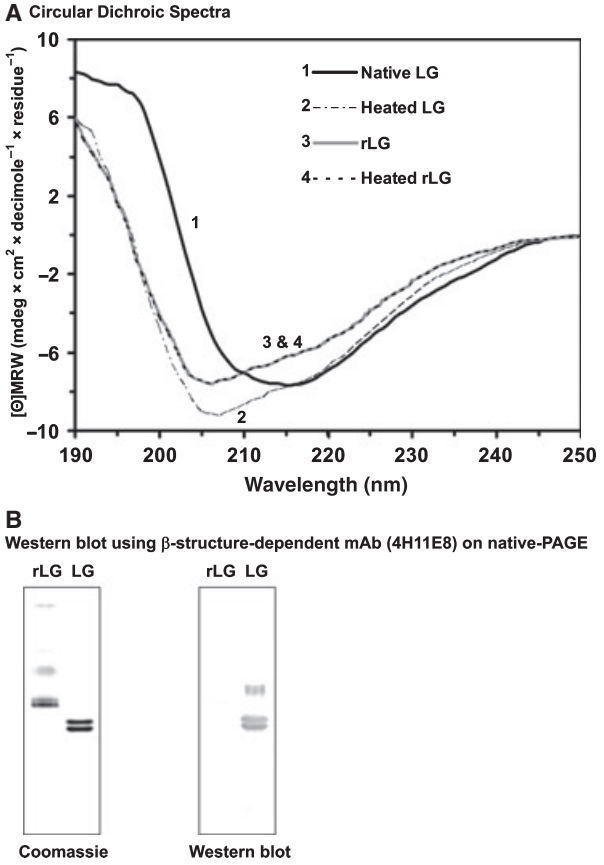

Fig. 5. CD and western blot analysis of rLG. (A) Native LG exhibits primarily a typical β-sheet conformation with a symmetrical dip at 215 nm. (B) MAb (4H11E8) specific for the native β-structure [8]. Western blot was performed using a 15% native PAGE.

the exosite (Fig. 1B,D), the presence of vitamin D_3 in the exosite is expected to interfere with the recognition of mAb 1D8F8, as depicted in our space-filling model (Fig. 7B). As Fig. 7C shows, the binding of vitamin D_3 to the 'exosite' of native LG, heated LG or rLG attenuated the recognition of mAb 1D8F8, according to a dot-blot assay, but, with the use of retinol and palmitate as a control, neither ligand affected the binding of 1D8F8. This result provides additional evidence for the involvement of the γ-turn loop in the binding of vitamin D.

Biological activity of LG in vitamin D_3 uptake in mice

To investigate whether LG binding to vitamin D can facilitate its uptake in an animal, we used the mouse as a model. We initially fed the animals ($n = 30$) with milk and milk fractions (LG, whey protein, or casein) all fortified with vitamin D_3 (final concentration 100 μM) for 3 weeks, and then determined the plasma intake of 25-hydroxyvitamin D (a metabolite of vitamin D). Figure 8A shows that the final mean concentrations of 25-hydroxyvitamin D in mice ($n = 5$ in each group) fed with raw milk, whey protein (without casein) or LG each supplemented with vitamin D_3 were significantly greater than those without LG (containing no LG) ($P < 0.001$). Casein, which lacks LG appears ineffective in the vitamin D uptake. The levels of 25-hydroxyvitamin D in all tested groups were elevated relative to the naive control without vitamin D_3 ($P < 0.001$).

Role of the exosite in uptake of vitamin D_3 in mice

To test the hypothesis that the exosite of LG plays a role in the transport of vitamin D, we compared the uptake of vitamin D_3 between native LG (containing a calyx and an exosite) and heated LG (containing only an exosite) as a strategy to evaluate their variation in uptake, if any [6,9]. Mice ($n = 65$) were separated into three major groups: those fed vitamin D_3 as a control (group 1), those fed LG supplemented with vitamin D_3 (group 2), and those fed heated LG supplemented with vitamin D_3 (group 3); mice fed with no vitamin D_3 were included as a baseline. Each subgroup of mice were then divided by increasing dosages of vitamin D_3 according to vitamin D_3/LG ratios (0.4, 1, 2, and 3), while LG or heated LG was maintained at a constant concentration (250 μM). Under these conditions, we expected to see the effect of the dosage of vitamin D_3 on its transport by the exosite. Figure 8B shows a typical dose response in all three major groups supplemented with vitamin D_3. Among these, the elevation of plasma 25-hydroxyvitamin D was prominent in group 2 (native LG supplemented with vitamin D_3). There seemed to be no saturation of 25-hydroxyvitamin D with vitamin D_3 at greater dosages in groups 2 and 3. When the values of the control group (group 1 fed vitamin D_3) were subtracted from those of groups 2 or 3, the levels of 25-hydroxyvitamin D appeared, remarkably, to be saturable (Fig. 8C). The dose–response curves fit exactly the binding ratios of vitamin D_3 versus LG; native LG containing two sites to bind vitamin D_3 hence produces maximal concentrations of plasma 25-hydroxyvitamin D at a dosage ratio of 2 : 1 (vitamin D_3/LG), whereas heated LG, containing only the exosite, produces maximal concentrations of plasma 25-hydroxyvitamin D at a dosage ratio of 1 : 1. The final increase in plasma 25-hydroxyvitamin D with native LG was almost exactly twice that of heated LG.

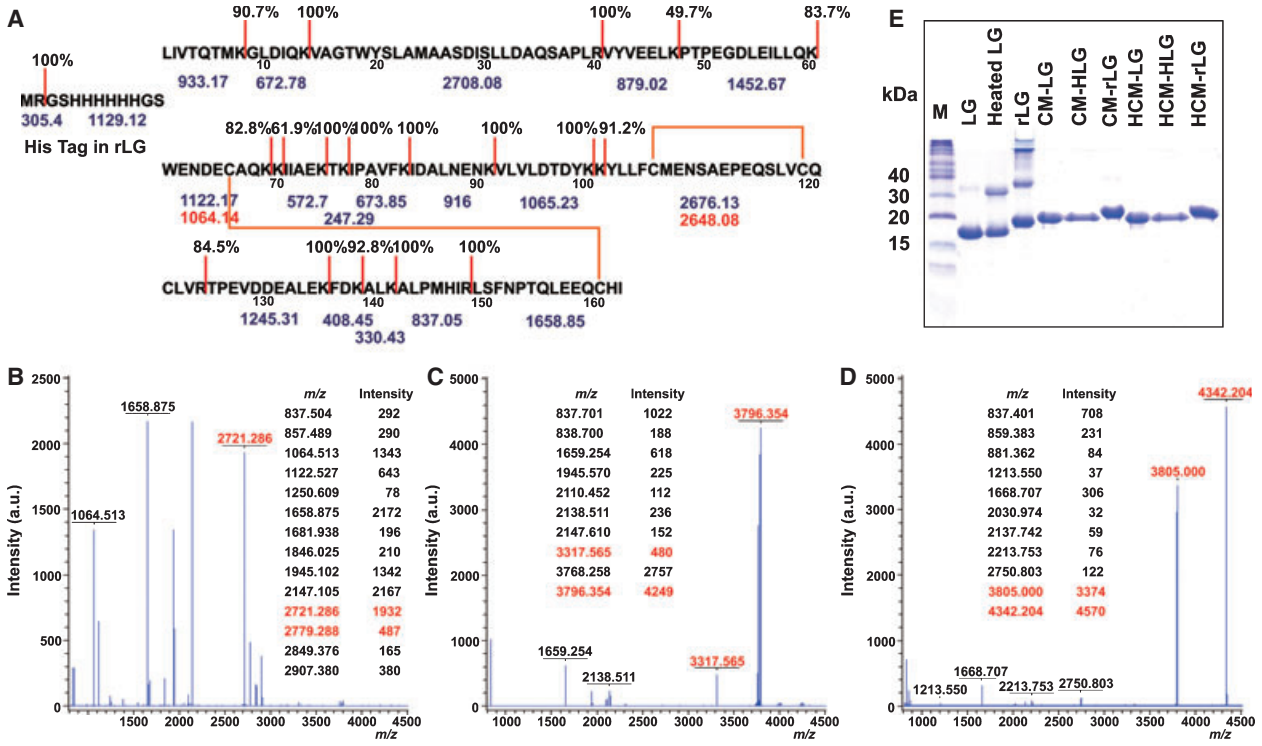

Fig. 6. MALDI-TOF MS analysis of trypsin-digested LG and carboxymethylation of LG. (A) Predicted trypsin cleavage sites (red bar, indicating cleavage probability) of LG isoform A obtained using a peptide cutter program (http://au.expasy.org/tools/peptidecutter/). The expected masses of peptide fragments (blue) and the disulfide linkages (orange bar) of native LG are depicted. LG isoform A with Asp64 and Val118 and isoform B with Gly64 and Ala118 in fragments 61–69 and 102–124 are shown in red. (B) MALDI-TOF spectrum of trypsin-digested native LG. Two mass spectra showing ions with *m/z* 2721.286 for isoform B and *m/z* 2779.288 for isoform A are representative for the fragment Trp61–Lys69:Leu149–Ile162 containing the disulfide linkage Cys66–Cys160. (C) Spectrum of trypsin-digested heated LG. Ions with *m/z* 3317.565 and *m/z* 3796.354 represent the dimeric Leu149–Ile162 and Trp61–Lys69:Tyr102–Arg124. (D) Spectrum of trypsin-digested rLG. Ions with *m/z* 3805.000 and *m/z* 4342.204 represent Trp61–Lys69:Tyr102–Arg124 and Tyr102–Arg124:Leu149–Ile162. (E) SDS/PAGE in the absence of mercaptoethanol of native LG, heated LG and rLG with or without carboxymethylation. HLG, CM and HCM denote heated LG, and carboxymethylated and heated carboxymethylated proteins, respectively. [Correction added on 18 March 2009 after first online publication: in the preceding sentence, 'with heat treatment' has been removed.] The molecular marker (M) is shown.

Table 2. Apparent dissociation constants and ratios for binding of vitamin D_3 to rLG and its γ-turn loop region mutants.

	Binding ratio calculated from Cogan plot (vitamin D_3/LG)	K_d^{app} Apparent dissociation constant (10^{-9} M)	Fold decrease in binding affinity
Wild-type	0.73 ± 0.03	33.1 ± 3.62[a]	
L143K	0.50 ± 0.02	301.1 ± 13.16	8.11
L143E	0.50 ± 0.02	226.3 ± 9.83	5.84
L143F	0.70 ± 0.02	64.8 ± 3.91	0.96
P144A	0.50 ± 0.02	185.3 ± 8.18	4.6
M145K	0.53 ± 0.02	208.6 ± 9.19	5.31
M145E	0.56 ± 0.02	189.8 ± 8.47	4.74
M145F	0.71 ± 0.02	59.7 ± 3.87	0.81

[a] $P < 0.001$ as compared to mutants. Data represent means of triplicate determinations.

Discussion

The major concern of this study is that the structure of rLG produced in *E. coli* no longer mimics that of native LG. We demonstrated, using MALDI-TOF analysis, that this phenomenon is due primarily to the mis-crosslinking of five Cys residues present in rLG (Fig. 6). rLG is composed of various dimeric and aggregated forms (Fig. 6E). Interestingly, however, following the irreversible reduction of all disulfide linkages by carboxymethylation, these forms become a homogeneous species similar to carboxymethylated LG. The same is seen with heated LG. We then showed that all carboxymethylated proteins lost a calyx, as they failed to interact with retinol and palmitate, but they still retained the ability to bind vitamin D_3, with a binding affinity almost identical

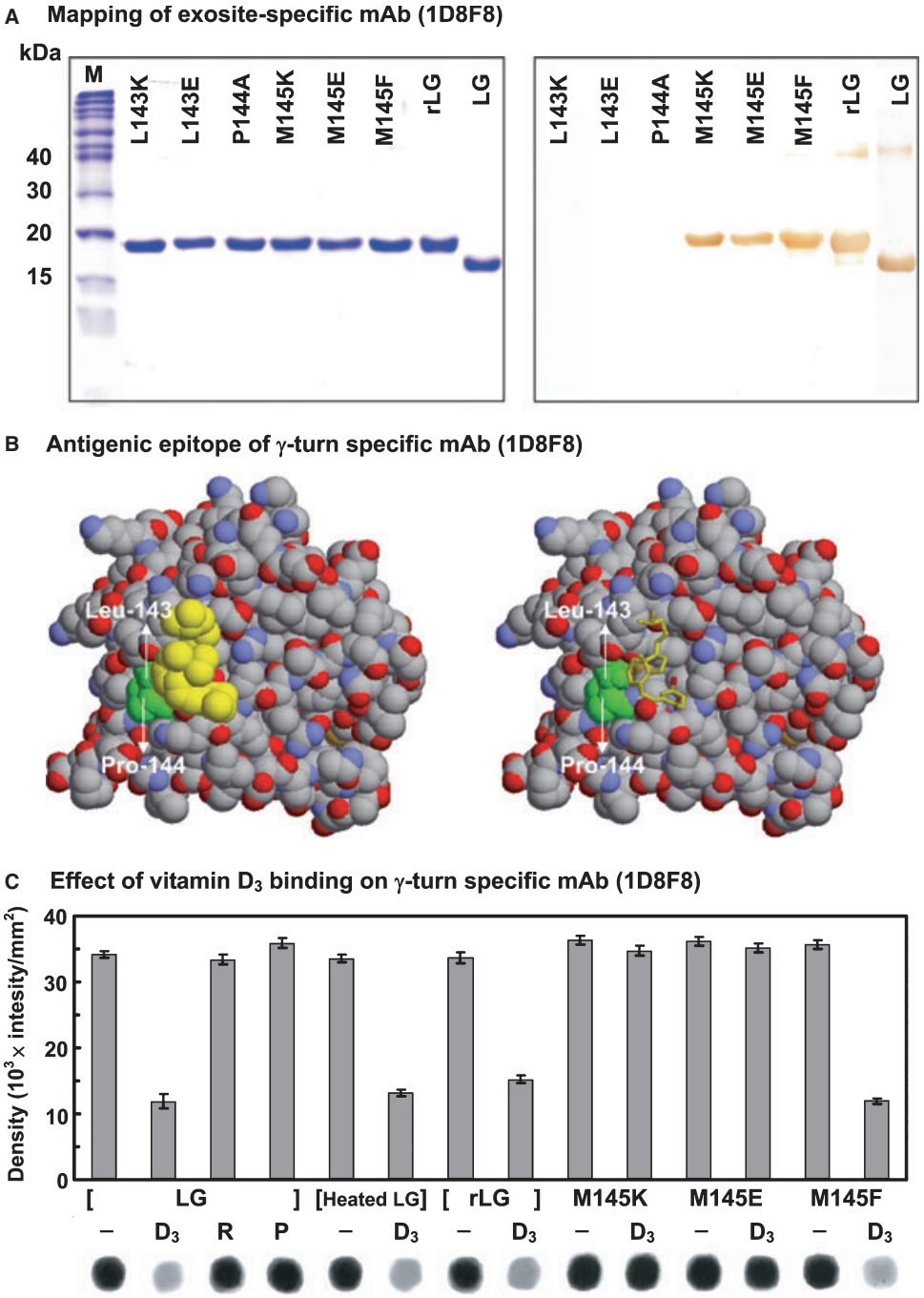

Fig. 7. Identification and epitope mapping of a γ-turn-specific mAb and the structure–function relationship between the γ-turn loop and vitamin D_3. (A) Identification of a mAb (1D8F8) specific for a γ-turn loop of LG, utilizing rLG mutants on a western blot. 1D8F8 recognizes native LG, rLG and some rLG mutants, but not mutants L143K, L143E, and P144A, indicating that γ-turn residues 143–144 are located within the epitope. (B) A space-filling model depicting residues 143 and 144 (green). They are within the vitamin D-binding exosite shared with 1D8F8. (C) Effect of vitamin D_3 binding on the immunoreactivity of LG, determined using dot-blot followed by scanning densitometric analysis (n = 3). R, P and D_3 represent retinol, palmitate and vitamin D_3, respectively.

to that of reduced LG or nonreduced rLG (Table 1). These data indicate that disulfide linkages of LG probably do not greatly affect the secondary binding to vitamin D. The reason for using heated LG in this study was as a control to evaluate exosite binding for rLG, because almost identical binding was found

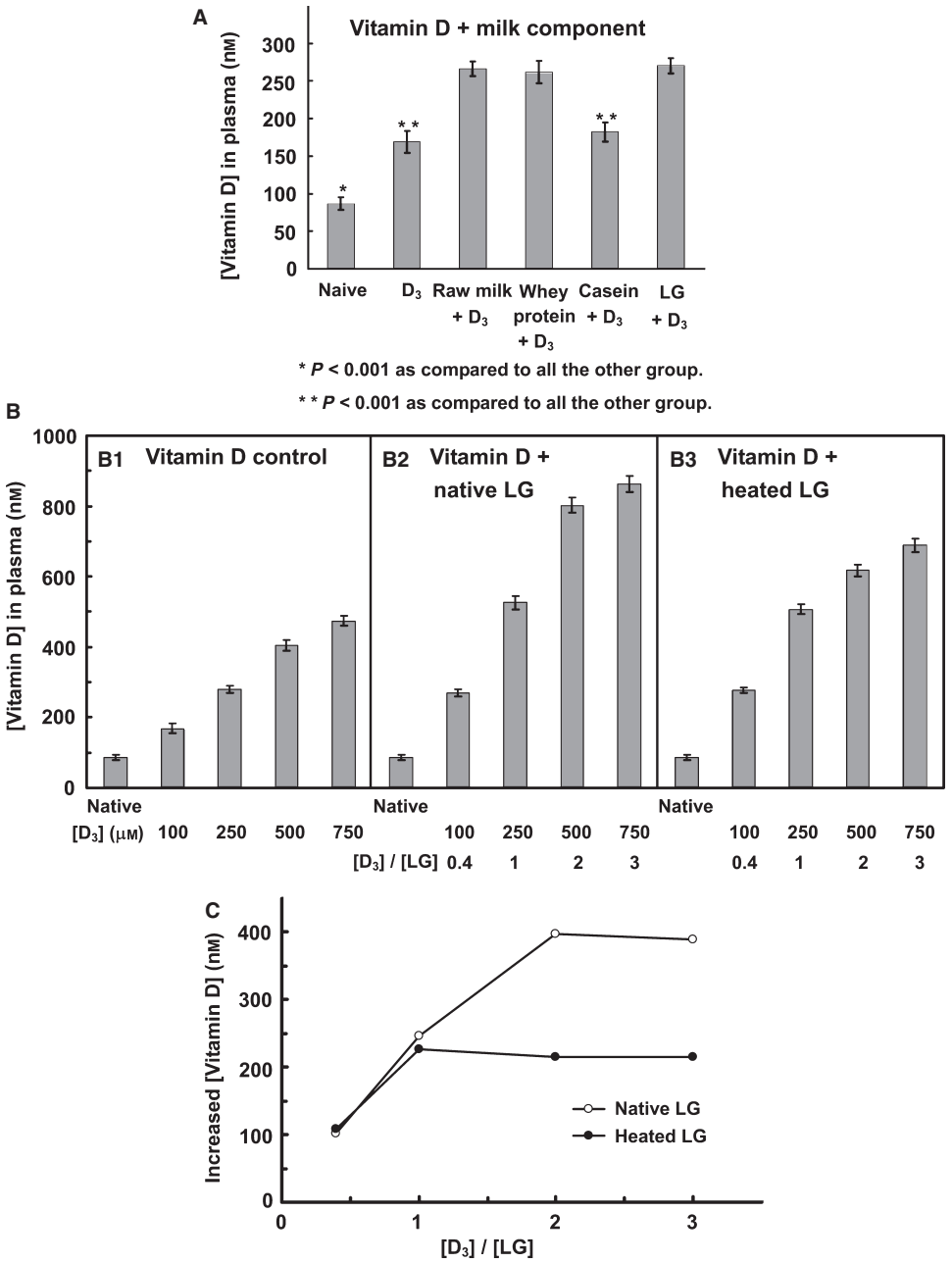

Fig. 8. Effect of LG on vitamin D_3 uptake in mice. (A) Concentration of 25-hydroxyvitamin D in plasma of mice fed (n = 5 for each group) with milk or its components supplemented with vitamin D_3 (100 μM). (B) Effect of native LG (containing the calyx and exosite) and heated LG (containing only the exosite) on uptake of vitamin D: each subgroup of mice (n = 5) was dosed with vitamin D_3 in groups 2 and 3 (0, 100, 250, 500 and 750 μM), according to the ratios 0, 0.4, 1, 2, and 3, respectively, of vitamin D_3/LG; vitamin D_3 alone (group 1) served as a control group. The concentration of LG was kept constant (250 μM). (C) Final 'adjusted' uptake of vitamin D after subtracting the values for the vitamin D_3 control group (group 1) from those for the vitamin D_3-fortified native LG (group 2) or the vitamin D_3-fortified heated LG group (group 3).

with rLG and heated rLG (Fig. 4A and Table 1). Whether the exosite of rLG maintains the same conformation as that of native LG is currently unknown. An ultimate solution is to obtain the crystal structure of the rLG–vitamin D complex, including the mutants, but at present we are unable to obtain a rLG–vitamin D crystal, probably because of the heterogeneous structures of rLG. We therefore subsequently used

the rLG mutants as a probe to investigate the importance of the γ-turn loop in vitamin D binding.

Another concern is that two Trp residues – Trp19 and Trp61 – in LG were involved when binding is monitored using fluorescence quenching. Several previous studies suggested that the intrinsic fluorescence of LG is due almost exclusively to Trp19 [24,25]. Trp19 is located at the bottom of the calyx, whereas Trp61 is more accessible to a solvent, and is thus able to make only a minor contribution to fluorescence emission [26]. On the basis of our previous studies [6,9,10], at pH 2–6 or after thermal treatment to switch off the gate of the calyx, we showed that vitamin D_3 interacted with only the exosite (with 35–40% of maximal binding ability), but not retinol and palmitate. The change of fluorescence caused by the binding of the exosite is 35–40% of that of the native LG containing two sites. The binding signal for the exosite is hence also attributed to Trp19, because Trp19 is located slightly away from the exosite. In addition, the fluorescence binding assay was conducted with a control (ethanol) and a blank (*N*-acetyl-L-tryptophanamide), to exclude the effects of a solvent and a ligand, respectively. Despite the small change in the fluorescence, Trp quenching in response to proximate ligand binding has served as a probe to investigate the dynamics of ligand and LG interactions [22].

Regardless of the undesired structural changes in *E. coli*-expressed LG, we provide several observations that might support the idea that the γ-turn loop plays a role in the interaction between the exosite and vitamin D [9]. First, substituting each Leu143 and Met145 with charged amino acids resulted in substantially decreased binding affinity of vitamin D_3 (4.7-fold to 8.1-fold in Table 2), which is consistent with a previous crystallographic report [9] showing the side chains of these two residues to be directly involved in vitamin D binding. It should be noted that these Leu and Met residues are projected into the interior of the protein, such that any mutation to charged residues would be highly disruptive of the structure of this loop; a change in vitamin D binding would therefore be expected. In contrast, such substitution might not greatly change the overall structure of the loop region, as demonstrated by the site-specific mAb 1D8F8 being able to recognize mutants M145K, M145E, and M145F (Fig. 7A). The substitution of centered Pro144 by Ala also significantly attenuated the binding affinity (4.6-fold in Table 2). Because Pro144 has no direct contact with vitamin D_3 [9], we suggest that it might be essential to maintain the conformation of the loop structure. All mutants other than L143F and M145F impaired vitamin D binding. There is a strong inverse correlation ($r = -0.94$) between the apparent dissociation constants and binding ratios for all mutants (Table 2). The binding ratios calculated from the Cogan plot are near 0.5 (Table 2), but the titration curve (Fig. 4, left panel) revealed that maximal binding was achieved at a ratio of 1 : 1. In general, the Cogan plot might indicate only that an impaired binding ratio might be caused by a markedly decreased binding affinity due to a unique structural change in those mutants. For example, the L143F and M145F mutants still showed a ratio of 0.7. Hence, Phe residues maintain the necessary hydrophobicity, although the overall conformation in this region might undergo some change.

Second, the exosites of rLG, heated LG, carboxymethylated LG, carboxymethylated rLG and carboxymethylated heated LG recognize only vitamin D_3, and neither palmitate nor retinol. This interaction appears to be ligand-specific and consistent with a previous study, in that there is no second binding site for palmitate and retinol [18]. Third, binding of vitamin D_3 to LG attenuated the recognition of a γ-turn loop-specific mAb (1D8F8) (Fig. 7).

With respect to the animal study, we found almost equal uptake of plasma 25-hydroxyvitamin D for mice dosed with equal concentrations of LG in vitamin D_3-fortified LG, whey protein (mainly LG and α-lactoalbumin), and raw milk (Fig. 8A). LG is therefore probably the only vehicle that transports vitamin D in milk. Interestingly, the use of LG supplemented with vitamin D_3 at various doses revealed that native LG, comprising two vitamin D-binding sites, produced maximal uptake of plasma vitamin D at a dosage ratio of 2 : 1 (vitamin D_3/LG), whereas heated LG, possessing only an exosite, produced maximal uptake of plasma vitamin D at a dosage ratio of 1 : 1 (Fig. 8). The final increase in plasma 25-hydroxyvitamin D caused by native LG was almost exactly twice that caused by heated LG. As a single mutation on the γ-turn loop (L143K) resulted in a maximal eight-fold decrease in binding affinity for vitamin D_3, it would be of interest to investigate the effect of such a mutation on the uptake of vitamin D in animals. This experiment is, however, impracticable at present, because of the limited quantity of rLG isolated in our expression system.

Increased concentrations of vitamin D in plasma have been demonstrated to be associated with a decreased incidence of breast, ovarian, prostate and colorectal cancers [27,28]. Because LG is a fraction that is directly responsible for enhancing the uptake of vitamin D in mice (Fig. 8), there might be two advantages of the presence of an exosite in LG. The first is that the central calyx of LG is thought to be partially occupied by fatty acid in milk [29]; the available

exosite might provide another route to transport vitamin D. Second, at present, the processing of many dairy products involves excessive heat for the purpose of sterilization. The presence of a thermally stable exosite might play a 'bypass' role in maintaining the binding and transport of vitamin D_3. Such a unique property of LG is worth considering for supplementing vitamin D in dairy products enriched with LG. It is worth mentioning here that mice and humans lack an LG gene [30]; the present finding indicates that vitamin D supplementation in milk (the biochemical event) is therefore essential for general public health. This is well worth following up in species that do express LG.

In summary, this study indicates a potential role of the γ-turn (Leu-Pro-Met) in maintaining the structure of a secondary vitamin D-binding site. The additional mouse experiment provides new insights into the transport role of LG and its supplementation with vitamin D used in dairy products.

Experimental procedures

Purification of native LG

LG was purified from raw milk using the supernatant from a saturated ammonium sulfate fraction (40%), followed by chromatography on a G-150 column, as described previously [5].

Analysis of the crystal structure of the LG–vitamin D_3 complex

The crystal structure of LG in this context is deposited in the Protein Data Bank, code 2GJ5 [9], and the diagram was created with Rasmol [31] and O v7.0 [32].

Construction of plasmid pQE30–LG

Total RNA was isolated from bovine mammary gland tissue; the cDNA was synthesized from RNA using M-MLV reverse transcriptase (Invitrogen, Carlsbad, CA, USA). The cDNA fragments coding for LG [33] were amplified on proofreading DNA polymerase (Invitrogen) and cloned into the *Bam*HI–*Hin*dIII sites of an *E. coli* expression vector, pQE30 (Qiagen, Madison, WI, USA). The plasmids were screened in JM109 and expressed in M15 (pREP4) (Qiagen), with the final sequence of pQE30–LG being confirmed by DNA sequencing [34,35].

Site-directed mutagenesis

Site-directed mutants ($n = 7$) of LG (L143K, L143E, L143F, M145K, M145E, M145F, and P144A) were generated using oligonucleotides containing the desired mutation with the QuikChange PCR method (Stratagene, La Jolla, CA, USA); the pQE30–LG expression vector served as a template [36], and the nucleotide sequence was confirmed. In addition, DNA nucleotide-sequencing analysis confirmed each inserted cDNA mutant of rLG to be correct.

Expression and purification of rLG and its mutants

E. coli [M15 (pREP4)] with pQE30–LG or its mutants were cultured in LB medium (containing 100 $\mu g \cdot mL^{-1}$ ampicillin and 1 mM isopropyl thio-β-D-galactoside) at 37 °C for 6 h on a rotary shaker. Cells were harvested at 8000 ***g*** for 20 min, resuspended in 40 mL of 20 mM Tris/HCl (pH 8.0), sonicated, and then centrifuged at 20 000 ***g*** for 20 min at 4 °C. The pellet containing inclusion bodies was resuspended in 30 mL of 2 M urea containing 20 mM Tris/HCl, 0.5 M NaCl, and 2% Triton X-100 (pH 8.0), sonicated as above, and then centrifuged at 20 000 ***g*** for 20 min at 4 °C. The inclusion bodies were then lysed, dissolved in a binding buffer containing 20 mM Tris/HCl, 0.5 M NaCl, 5 mM imidazole, 6 M guanidine-HCl, and 1 mM 2-mercaptoethanol (pH 8.0), and passed through a syringe filter (0.45 μm). A HiTrap chelating column (GE Healthcare, Uppsala, Sweden) was washed with 0.1 M $NiSO_4$ and equilibrated with the binding buffer before the cell lysate was loaded as previously described [35]. The column-bound fraction was then treated with a binding buffer containing 6 M urea, and finished with the binding buffer without urea. The recombinant protein was finally eluted with a buffer containing 20 mM Tris/HCl, 0.5 M NaCl, and 250 mM imidazole without 2-mercaptoethanol (pH 8.0). Protein fractions were pooled, desalted on a P-2 column (Bio-Rad laboratories, Hercules, CA, USA), and lyophilized. The protein concentration was determined by the Lowry method [37], using BSA as a standard.

Gel electrophoresis and immunoblot analysis

SDS/PAGE or native PAGE with 15% polyacrylamide gel was used to characterize rLG and its mutants, using a modified procedure similar to that described previously [7,38]. The samples for SDS/PAGE or native PAGE were mixed with a loading buffer (12 mM Tris/HCl, 0.4% SDS, 5% glycerol, and 0.02% bromphenol blue, pH 6.8) without thermal treatment to ensure the retention of the native structure of LG. For reducing PAGE, mercaptoethanol at a final concentration of 143 mM in the samples was used. Western blot analysis was performed as described previously [6]: the electrotransferred samples were incubated with mAbs (4D11, 4H11E8, or 1D8F8) [5], and developed using 3,3′-di-aminobenzidine containing 0.01% H_2O_2 [6]. Dot-blot to assess the interaction between vitamin D_3 and

the exosite was performed using the samples of LG or LG–vitamin D_3 complex (ratio 1 : 10) spotted onto the membrane; the final binding was probed with a γ-loop-specific mAb (1D8F8).

Vitamin D_3 binding to LG, rLG and rLG mutants

The ligand-binding assay for LG was performed with fluorescence emission as previously established [6,9,10,21,22,24,25]. The binding of vitamin D_3 to LG was measured by fluorescence quenching of Trp19 of LG at 332 nm, using excitation at 287 nm. Fluorescence spectra (Cary Eclipse fluorescence spectrophotometer; Varian Inc., Palo Alto, CA, USA) were recorded at 24 °C. For the titration experiment, 5 μM native LG, heated LG (preheated at 100 °C for 16 min), rLG or its mutants (in 10 mM phosphate buffer, pH 8.0) was instantly incubated with increased concentrations of vitamin D_3 (0.625–20 μM in absolute ethanol). The final concentration of ethanol in the reaction mixture was such that it was < 3% at the endpoint of the titration. With this concentration, neither aggregation of LG nor a significant change in fluorescence emission was produced [39,40]. As in previous studies [6,9,10,21,22,25], the titration of LG protein with various concentrations of ethanol (up to 3%) was evaluated and employed as an initial intrinsic fluorescence of LG before the addition of ligands. A solution of *N*-acetyl-L-tryptophanamide (Sigma-Aldrich, St Louis, MO, USA), with an absorbance at 287 nm that was equal to that of the tested protein, was also used as a blank during the ligand titration, according to the method previously established [21,22,25]. The decreased intensity of fluorescence of *N*-acetyl-L-tryptophanamide solution during the titration was thus not due to the interaction between ligand and tryptophanamide, but resulted from the inner filter effect as a consequence of ligand absorbance at 287 nm [41]. The change in fluorescence intensity at 332 nm depended on the amount of protein–ligand complex, allowing the calculation of a (the fraction of unoccupied ligand-binding sites), using the equation $a = (F - F_{sat})/(F_0 - F_{sat})$ as previously described [21,22,25]. The data were then transformed to a plot of the Cogan equation, $(P_T a = (1/n)[R_T a/(1 - a)] - K_d^{app}/n)$, in which P_T is the total protein concentration, n is the number of binding sites per molecule, R_T is the total ligand concentration, and K_d^{app} is the apparent dissociation constant [42].

CD

For CD measurement, 0.5 mg·mL^{-1} of native or heated LG (100 °C for 16 min), rLG or its mutants (in 20 mM phosphate buffer, pH 7.0) was added to a cuvette of 1.0 mm path length [9,38]. The CD spectra were recorded 20 times on a Jasco-J715 spectropolarimeter (Jasco, Tokyo, Japan) at 24 °C over the range from 200 to 250 nm at a scan speed of 20 nm·min^{-1}.

MALDI-TOF MS analysis of trypsin-digested LG

For trypsin treatment, 100 μg of LG, heated LG or rLG in 50 μL of NaCl/P_i containing 0.02 M phosphate and 0.12 M NaCl (pH 7.4) was incubated with 1 μL of trypsin (0.5 mg·mL^{-1}) at 37 °C for 16 h. The reaction was terminated by adding 1 mM phenylmethanesulfonyl fluoride. The trypsinized samples were then concentrated using C18 Zip-Tips and eluted with 50% acetonitrile/0.1% trifluroacetic acid following the manufacturer's (Millipore, Billerica, MA, USA) standard protocol. MALDI-TOF MS was performed using a Microflex MALDI-TOF LRF20 mass spectrometer (Bruker Daltonics, Billerica, MA, USA). The Zip-Tips-purified peptide digests were spotted with an α-cyano-4-hydroxycinnamic acid matrix and run in reflectron positive-ion mode at an accelerating voltage of 25 kV.

Carboxymethylation of LG

For carboxymethylation [6,8,38], 5 mg of LG, heated LG or rLG was first dissolved in 2 mL of 0.1 M Tris/HCl buffer (pH 8.6), containing 6 M ultrapure urea and 0.02 M dithiothreitol. Following flushing with nitrogen for 2 h, 20 mg of iodoacetic acid was added to the reaction mixture, while the pH was maintained at 8.6 by the addition of 0.1 M NaOH, and incubation was performed for another 3 h. Finally, carboxymethylated LG, carboxymethylated heated LG and carboxymethylated rLG were desalted on a Bio-Gel P2 column, eluted with 0.05 M ammonium bicarbonate, and lyophilized.

Animal experiments

Female BALB/c mice (4 weeks old, $n = 95$, obtained from the National Animal Center, National Science Council of Taiwan) were kept in an animal room (12 h light cycle, 21 °C) and fed with a standard diet; housing and management were according to guidelines established and approved by the National Science Council of Taiwan. In an initial test using milk fortified with vitamin D_3 and fortified milk components, mice ($n = 30$) with body mass 17.56 ± 1.28 g [mean ± standard deviation (SD)] were randomly divided into six groups ($n = 5$). Vitamin D_3 (100 μM) was emulsified with raw milk, whey protein (milk without casein), casein (reconstituted to the milk volume), LG (250 μM, approximately equivalent to the concentration in milk) or distilled water in a feeding bottle (*ad libitum*), and mice were fed with this for 3 weeks. Each mouse drank ~ 3–3.5 mL·day^{-1} on average. The mean body mass of each group increased by 8% in general, and there was no significant difference among the groups at the end of the test. For the experimental dosing with vitamin D_3, mice ($n = 65$, with body mass 17.73 ± 1.17 g, mean ± SD) were divided into three major groups: group 1 (vitamin D_3), group 2 (vitamin D_3 plus native LG), and

group 3 (vitamin D_3 plus heated LG). The experiment was designed to investigate the relationship between the vitamin D-binding sites of LG and the uptake of vitamin D. LG serving as a vehicle was kept at a constant concentration (250 μM) during the feeding period. Group 1 ($n = 20$) without LG was dosed with only vitamin D_3, as a control. All groups were given varied dosages: 100, 250, 500 or 750 μM vitamin D_3 according to vitamin D_3/LG ratios of 0.4, 1, 2, or 3, respectively. Group 2 ($n = 20$) and group 3 ($n = 20$) were provided with native LG (containing two binding sites) and heated LG (containing one binding site), respectively. As well as these three groups, one naive group given no vitamin D_3 and LG was included ($n = 5$). Preparation of the vitamin D_3 supplement and the protocol (3 weeks) were as described above. Analysis of 25-hydroxyvitamin D in mouse plasma was conducted with a kit (25-Hydroxy Vitamin D Direct EIA; IDS Diagnostics, Fountain Hills, AZ, USA), according to the manufacturer's instructions.

Acknowledgements

This work was supported by National Science Council (NSC) grants 92-2313-B-009-002, 93-2313-B009-002, 94-2313-B-009-001, 95-2313-B-009-001, and 97-2313-B-009-001-MY2 (S. J. T. Mao), and NSC 94-2321-B-213-001, 95-2321-B-213-001-M (NSC), 963RSB02, and 973RSB02 (National Synchrotron Radiation Research Center) (C.-J. Chen).

References

1 Hambling SG, MacAlpine AS & Sawyer L (1992) Beta-lactoglobulin. In *Advanced Dairy Chemistry I* (Fox PF, eds), pp. 141–190. Elsevier, Amsterdam.
2 Sawyer L & Kontopidis G (2000) The core lipocalin, bovine beta-lactoglobulin. *Biochim Biophys Acta* **1482**, 136–148.
3 Marshall K (2004) Therapeutic applications of whey protein. *Altern Med Rev* **9**, 136–156.
4 Sava N, Van der Plancken I, Claeys W & Hendrickx M (2005) The kinetics of heat-induced structural changes of beta-lactoglobulin. *J Dairy Sci* **88**, 1646–1653.
5 Chen WL, Huang MT, Liu HC, Li CW & Mao SJT (2004) Distinction between dry and raw milk using monoclonal antibodies prepared against dry milk proteins. *J Dairy Sci* **87**, 2720–2729.
6 Song CY, Chen WL, Yang MC, Huang JP & Mao SJT (2005) Epitope mapping of a monoclonal antibody specific to bovine dry milk: involvement of residues 66–76 of strand D in thermal denatured beta-lactoglobulin. *J Biol Chem* **280**, 3574–3582.
7 Chen WL, Hwang MT, Liau CY, Ho JC, Hong KC & Mao SJT (2005) β-Lactoglobulin is a thermal marker in processed milk as studied by electrophoresis and circular dichroic spectra. *J Dairy Sci* **88**, 1618–1630.
8 Chen WL, Liu WT, Yang MC, Hwang MT, Tsao JH & Mao SJT (2006) A novel conformation-dependent monoclonal antibody specific to the native structure of beta-lactoglobulin and its application. *J Dairy Sci* **89**, 912–921.
9 Yang MC, Guan HH, Liu MY, Lin YH, Yang JM, Chen WL, Chen CJ & Mao SJT (2008) Crystal structure of a secondary vitamin D_3 binding site of milk beta-lactoglobulin. *Proteins* **71**, 1197–1210.
10 Yang MC, Guan HH, Yang JM, Ko CN, Liu MY, Lin YH, Huang YC, Chen CJ & Mao SJT (2008) Rational design for crystallization of β-lactoglobulin and vitamin D_3 complex: revealing a secondary binding site. *Cryst Growth Des* **8**, 4268–4276.
11 Qin BY, Bewley MC, Creamer LK, Baker EN & Jameson GB (1999) Functional implications of structural differences between variants A and B of bovine beta-lactoglobulin. *Protein Sci* **8**, 75–83.
12 Greene LH, Hamada D, Eyles SJ & Brew K (2003) Conserved signature proposed for folding in the lipocalin superfamily. *FEBS Lett* **553**, 39–44.
13 Lüthy R, Bowie JU & Eisenberg D (1992) Assessment of protein models with three-dimensional profiles. *Nature* **356**, 83–85.
14 Kontopidis G, Holt C & Sawyer L (2004) Invited review: beta-lactoglobulin: binding properties, structure, and function. *J Dairy Sci* **87**, 785–796.
15 Adams JJ, Anderson BF, Norris GE, Creamer LK & Jameson GB (2006) Structure of bovine beta-lactoglobulin (variant A) at very low ionic strength. *J Struct Biol* **154**, 246–254.
16 Bello M, Pérez-Hernández G, Fernández-Velasco DA, Arreguín-Espinosa R & García-Hernández E (2008) Energetics of protein homodimerization: effects of water sequestering on the formation of beta-lactoglobulin dimer. *Proteins* **70**, 1475–1487.
17 Wu SY, Perez MD, Puyol P & Sawyer L (1999) Beta-lactoglobulin binds palmitate within its central cavity. *J Biol Chem* **274**, 170–174.
18 Kontopidis G, Holt C & Sawyer L (2002) The ligand-binding site of bovine beta-lactoglobulin: evidence for a function? *J Mol Biol* **318**, 1043–1055.
19 Considine T, Singh H, Patel HA & Creamer LK (2005) Influence of binding of sodium dodecyl sulfate, all-trans-retinol, and 8-anilino-1-naphthalenesulfonate on the high-pressure-induced unfolding and aggregation of beta-lactoglobulin B. *J Agric Food Chem* **53**, 8010–8018.
20 Konuma T, Sakurai K & Goto Y (2007) Promiscuous binding of ligands by beta-lactoglobulin involves hydrophobic interactions and plasticity. *J Mol Biol* **368**, 209–218.

21 Wang Q, Allen JC & Swaisgood HE (1999) Binding of lipophilic nutrients to beta-lactoglobulin prepared by bioselective adsorption. *J Dairy Sci* **82**, 257–264.
22 Wang Q, Allen JC & Swaisgood HE (1997) Binding of vitamin D and cholesterol to beta-lactoglobulin. *J Dairy Sci* **80**, 1054–1059.
23 Kuwata K, Shastry R, Cheng H, Hoshino M, Batt CA, Goto Y & Roder H (2001) Structural and kinetic characterization of early folding events in β-lactoglobulin. *Nat Struct Biol* **8**, 151–155.
24 Cho Y, Batt CA & Sawyer L (1994) Probing the retinol-binding site of bovine beta-lactoglobulin. *J Biol Chem* **269**, 11102–11107.
25 Wang Q, Allen JC & Swaisgood HE (1997) Binding of retinoids to beta-lactoglobulin isolated by bioselective adsorption. *J Dairy Sci* **80**, 1047–1053.
26 Brownlow S, Morais Cabral JH, Cooper R, Flower DR, Yewdall SJ, Polikarpov I, North AC & Sawyer L (1997) Bovine beta-lactoglobulin at 1.8 A resolution – still an enigmatic lipocalin. *Structure* **5**, 481–495.
27 Vieth R (2001) Vitamin D nutrition and its potential health benefits for bone, cancer and other conditions. *J Nutr Environ Med* **11**, 275–291.
28 Lappe JM, Travers-Gustafson D, Davies KM, Recker RR & Heaney RP (2007) Vitamin D and calcium supplementation reduces cancer risk: results of a randomized trial. *Am J Clin Nutr* **85**, 1586–1591.
29 Pérez MD, Díaz de Villegas C, Sánchez L, Aranda P, Ena JM & Calvo M (1989) Interaction of fatty acids with beta-lactoglobulin and albumin from ruminant milk. *J Biochem* **106**, 1094–1097.
30 Simons JP, McClenaghan M & Clark AJ (1987) Alteration of the quality of milk by expression of sheep beta-lactoglobulin in transgenic mice. *Nature* **328**, 530–532.
31 Sayle RA & Milner-White EJ (1995) RASMOL: biomolecular graphics for all. *Trends Biochem Sci* **20**, 374–376.
32 Jones TA, Zou JY, Cowan SW & Kjeldgaard M (1991) Improved methods for building protein models in electron density maps and the location of errors in these models. *Acta Crystallogr A* **47**, 110–119.
33 Jamieson AC, Vandeyar MA, Kang YC, Kinsella JE & Batt CA (1987) Cloning and nucleotide sequence of the bovine beta-lactoglobulin gene. *Gene* **61**, 85–90.
34 Lai IH, Tsai TI, Lin HH, Lai WY & Mao SJT (2007) Cloning and expression of human haptoglobin subunits in *Escherichia coli*: delineation of a major antioxidant domain. *Protein Expr Purif* **52**, 356–362.
35 Lai IH, Lin KY, Larsson M, Yang MC, Shiau CH, Liao MH & Mao SJT (2008) A unique tetrameric structure of deer plasma haptoglobin – an evolutionary advantage in the Hp 2-2 phenotype with homogeneous structure. *FEBS J* **275**, 981–993.
36 Ju M, Stevens L, Leadbitter E & Wray D (2003) The roles of N- and C-terminal determinants in the activation of the Kv2.1 potassium channel. *J Biol Chem* **278**, 12769–12778.
37 Lowry OH, Rosebrough NJ, Farr AL & Randall RJ (1951) Protein measurement with the Folin phenol reagent. *J Biol Chem* **193**, 265–275.
38 Tseng CF, Lin CC, Huang HY, Liu HC & Mao SJT (2004) Antioxidant role of human haptoglobin. *Proteomics* **4**, 2221–2228.
39 Dufour E & Haertlé T (1990) Alcohol-induced changes of beta-lactoglobulin retinol-binding stoichiometry. *Protein Eng* **4**, 185–190.
40 Dufour E, Genot C & Haertlé T (1994) beta-Lactoglobulin binding properties during its folding changes studied by fluorescence spectroscopy. *Biochim Biophys Acta* **1205**, 105–112.
41 Dufour E & Haertlé T (1991) Binding of retinoids and beta-carotene to beta-lactoglobulin. Influence of protein modifications. *Biochim Biophys Acta* **1079**, 316–320.
42 Cogan U, Kopelman M, Mokady S & Shinitzky M (1976) Binding affinities of retinol and related compounds to retinol binding proteins. *Eur J Biochem* **65**, 71–78.